



Title	Anomalous behaviors of E1 E2 deep level defects in 6H silicon carbide
Author(s)	Chen, XD; Ling, CC; Gong, M; Fung, S; Beling, CD; Brauer, G; Anwand, W; Skorupa, W
Citation	Applied Physics Letters, 2005, v. 86 n. 3, p. 1-3
Issued Date	2005
URL	http://hdl.handle.net/10722/42230
Rights	Creative Commons: Attribution 3.0 Hong Kong License

Anomalous behaviors of E_1/E_2 deep level defects in 6H silicon carbide

X. D. Chen and C. C. Ling^{a)}

Department of Physics, The University of Hong Kong, Pokfulam Road, Hong Kong, People's Republic of China

M. Gong

Department of Physics, Sichuan University, Chengdu, People's Republic of China

S. Fung and C. D. Beling

Department of Physics, The University of Hong Kong, Pokfulam Road, Hong Kong, People's Republic of China

G. Brauer, W. Anwand, and W. Skorupa

Institut für Ionenstrahlphysik und Materialforschung, Forschungszentrum Rossendorf, Postfach 510119, D-01314 Dresden, Germany

(Received 24 May 2004; accepted 22 November 2004; published online 7 January 2005)

Deep level defects E_1/E_2 were observed in He-implanted, 0.3 and 1.7 MeV electron-irradiated n -type 6H-SiC. Similar to others' results, the behaviors of E_1 and E_2 (like the peak intensity ratio, the annealing behaviors or the introduction rates) often varied from sample to sample. This anomalous result is not expected of E_1/E_2 being usually considered arising from the same defect located at the cubic and hexagonal sites respectively. The present study shows that this anomaly is due to another DLTS peak overlapping with the E_1/E_2 . The activation energy and the capture cross section of this defect are $E_C=0.31$ eV and $\sigma\sim 8\times 10^{-14}$ cm², respectively. © 2005 American Institute of Physics. [DOI: 10.1063/1.1853523]

Silicon carbide (SiC) is a wide band-gap semiconductor material having physical and electronic properties suitable for high-temperature, high-power, and high-frequency electronic applications.¹ Deep level defects induced by ion implantation or particle irradiation in SiC have been extensively studied by capacitance transient techniques such as deep level transient spectroscopy (DLTS).²⁻¹¹ Deep levels E_1/E_2 ($E_C=0.34$ eV/0.44 eV) are dominant levels observed in electron-irradiated n -type 6H-SiC^{3-6,8,10} (known as Z_1/Z_2 in 4H-SiC). However, their intensities are relatively low in neutron irradiated or He implanted samples.^{2,3,9} E_1/E_2 are usually considered to be the same defect but residing at the hexagonal (h) and the cubic (k_1, k_2) sites, respectively. This implies that their physical behaviors such as the peak intensity ratio, introduction rates and annealing behaviors, should be independent of sample. However, observations have indicated otherwise.^{4,5} To investigate this anomaly, we have performed DLTS and annealing studies on He-implanted and electron-irradiated (with energies $E_e=0.2, 0.3$, and 1.7 MeV) 6H-SiC.

The starting n -type materials were 5- μ m-nitrogen doped (0001) epitaxial layer ($n=1\times 10^{16}$ cm⁻³) grown on n^+ -type 6H-SiC substrate ($n=8\times 10^{17}$ cm⁻³) purchased from Cree Inc. Details of sample preparation, Ohmic and Schottky contacts fabrication were reported in Ref. 9. Samples were implanted with He ions and irradiated with electrons to create the E_1/E_2 defects. He ions with energies of 55, 210, 430, 665, and 840 keV (each with fluence of $\sim 2\times 10^{11}$ cm⁻²) were implanted into the sample so as to produce a 2 μ m deep box-shape implanted layer. Electron irradiation was carried out with electrons energies of 1.7, 0.3, and 0.2 MeV (dosage 5×10^{15} cm⁻²). Isochronal annealing from

100 to 1200 °C was carried out in the Ar gas atmosphere for 30 min. The quality of all the Schottky-diode-like samples were monitored by observing $I-V$ and $C-V$ characteristics. DLTS was carried out at 100–400 K.

Figure 1 shows DLTS spectra of the He-implanted, electron-irradiated ($E_e=0.3$ and 1.7 MeV) samples with different annealing treatments. The E_1/E_2 peaks (at ~ 200 K) were the dominant peaks in the as-electron-irradiated samples. However, these were not detected in the 0.2 MeV electron-irradiated sample.¹⁰ Moreover, these peaks from the as-1.7-MeV-irradiated sample shift to the low temperature side and the line shape was also broadened as compared to the 0.3 MeV sample.¹⁰ However, with annealing above 300 °C, these peaks for the 1.7 MeV sample become narrower and the position shift to the high temperature side¹⁰

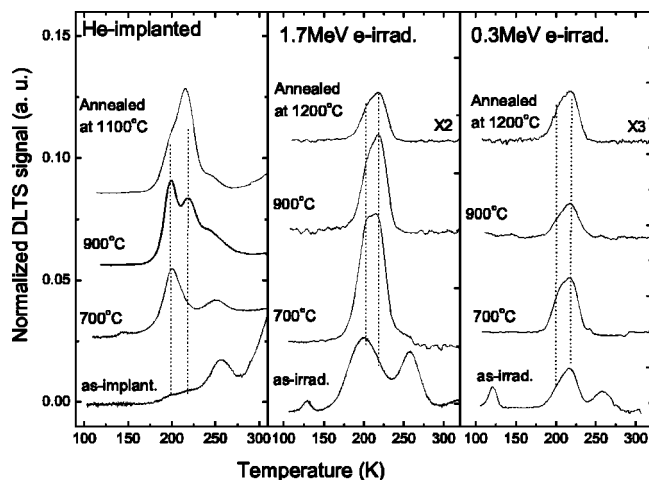


FIG. 1. DLTS spectra for the He-implanted, 1.7 and 0.3 MeV electron-irradiated samples with different annealing conditions. A rate window of 6.82 ms was used in the measurements.

^{a)}Electronic mail: ccling@hku.hk

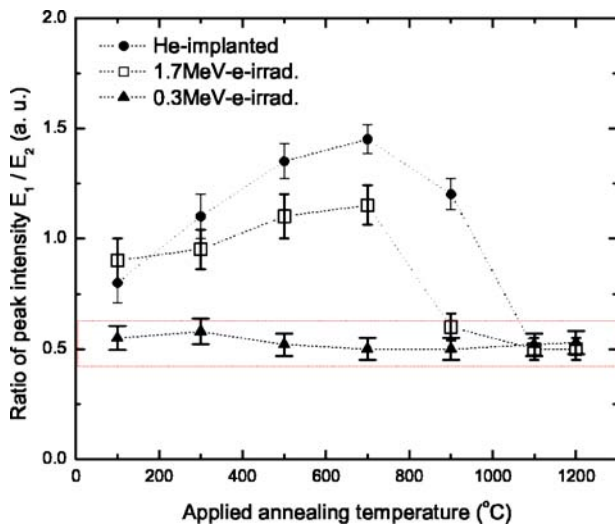


FIG. 2. Peak intensities of E_1/E_2 as a function of annealing temperature for the He-implanted, 0.3 and 1.7 MeV electron-irradiated samples.

(see the 700 °C annealed 1.7 MeV electron-irradiated spectrum in Fig. 1). This observation is ascribed to the presence of another deep level peak ED2 on the low temperature side of the E_1 . ED2 was only introduced with $E_e \geq 0.5$ MeV and is annealed out at 300 °C.¹⁰ In contrast, the E_1/E_2 signal was very weak in the as-He-implanted sample and strengthened with increasing annealing temperature.

Figure 2 shows the $E_1:E_2$ intensities ratio as a function of annealing temperature T_a for different samples. If E_1/E_2 are the same defect at the h and two k sites, their intensity ratio should thus be fixed and annealing behavior similar. For the 0.3 MeV irradiated sample, the $E_1:E_2$ ratio was constant at ~ 0.5 for the whole range of annealing temperatures. However, for the 1.7-MeV-irradiated and the He-implanted samples, different $E_1:E_2$ ratios (~ 0.8 – 1.3) were observed at $T_a = 100$ °C and they increase with increasing T_a (< 700 °C). They then decrease towards a constant value of ~ 0.5 (which is the same as the 0.3 MeV electron-irradiated sample) after the ~ 1000 °C annealing. This clearly shows that, for 100–900 °C, the annealing behaviors of E_1 and E_2 are quite different for these samples. Different $E_1:E_2$ ratios have also been reported in previous literature.^{4,5,8,11}

The peak intensity increases with the filling pulse width t_p as: $\Delta C(t_p) = \Delta C(t_p \rightarrow \infty)(1 - \exp[-\sigma n v t_p])$, where n is the free carrier concentration and v the carrier thermal velocity. By plotting $\ln[1 - \Delta C(t_p)/\Delta C(t_p = 1 \text{ ms})]/n v$ against t_p , a straight line should be obtained and the majority carrier capture cross-section σ of E_1/E_2 can be determined from the slope. Figure 3 shows the spectra and E_1/E_2 intensities of the 0.3 and 1.7 MeV as-irradiated samples taken with different t_p . For the 0.3 MeV sample, the E_1/E_2 peaks maintains similar shape and the expected straight lines in the log plot yield $\sigma(E_1) \sim \sigma(E_2) \sim 1 - 5 \times 10^{-15} \text{ cm}^2$. However, for the 1.7 MeV sample, the intensity of E_1 is larger than that of E_2 at short t_p , but it becomes smaller than that of E_2 with long t_p (as illustrated in the DLTS spectra and the log plot in Fig. 3). The straight line of the E_2 's data log plot yields $\sigma(E_2) = 2 - 6 \times 10^{-15} \text{ cm}^2$, which is similar to those of E_1 and E_2 found in the 0.3 MeV irradiated sample. However, the log plot of the E_1 does not yield a straight line. These anomalous effects would not be observed if E_1 and E_2 were identical defects occupying different equivalent lattice sites as their

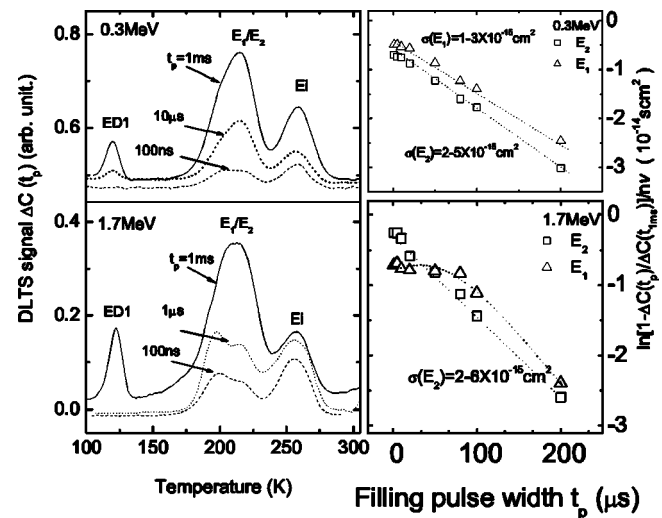


FIG. 3. DLTS spectra (left) and peak intensities (right) of E_1 and E_2 of the 1.7 and 0.3 MeV as-electron-irradiated samples as a function of filling pulse width t_p .

properties should have the similar t_p dependence. The anomaly was also observed in the as-He-implanted samples. Moreover, the anomalies in the He implanted and the 1.7 MeV e^- -irradiated samples disappear after annealing at about 1000 °C.

First, we can conclude that the anomalies are not associated with ED2 which overlaps with the E_1/E_2 peaks because the ED2 has already annealed out at 300 °C. Moreover, these anomalies were not observed in the low energy irradiated (0.3 MeV) samples or after 1000 °C annealing. One plausible explanation for such observations is the presence of an extra DLTS peak which overlaps with the E_1/E_2 peaks. This defect, which anneals out at about 1000 °C, is induced by He implantation or with electron irradiation with energy as high as 1.7 MeV. This implies that the E_1/E_2 peaks observed in the low energy electron-irradiated (0.3 MeV) sample, the 1.7 MeV irradiated and the He-implanted samples after the 1000 °C annealing are the “pure” E_1/E_2 peaks. From all these spectra which contain the “pure” E_1/E_2 peaks, $\sigma(E_1) \sim \sigma(E_2) \sim 5 \times 10^{-15} \text{ cm}^2$ and $E_1:E_2$ ratio is ~ 0.5 . As the E_1 signal observed in the He implanted and the 1.7 MeV electron irradiated samples annealed at temperatures below 1000 °C is contributed from the pure E_1 and the proposed extra defect, the different annealing behaviors of the E_1 and E_2 peak intensities as seen in Figs. 1 and 2, and also the anomalous log plot shown in Fig. 3 can thus be understood.

In order to test our proposed phenomena that the proposed defect peak merged with the E_1/E_2 signals and were too close to be well separated (as shown in Fig. 1), we have attempted to resolved the proposed peak and the E_1/E_2 by changing the spectrometer's settings (i.e., V_R , rate window and t_p) as varying these settings would change the peaks positions and intensities, and the extent of change would vary from defect to defect. Figure 4 shows the most convincing evidence for our proposal, in which the proposed peak was clearly seen in the DLTS spectrum of the 900 °C He implanted sample with $V_R = -2$ V, rate window = 136 ms and $t_p = 100 \mu\text{s}$. Here the proposed defect peak is clearly separated with the E_1 peak. This peak can be observed with the rate window = 136 ms but not in the spectra in Fig. 1 (rate

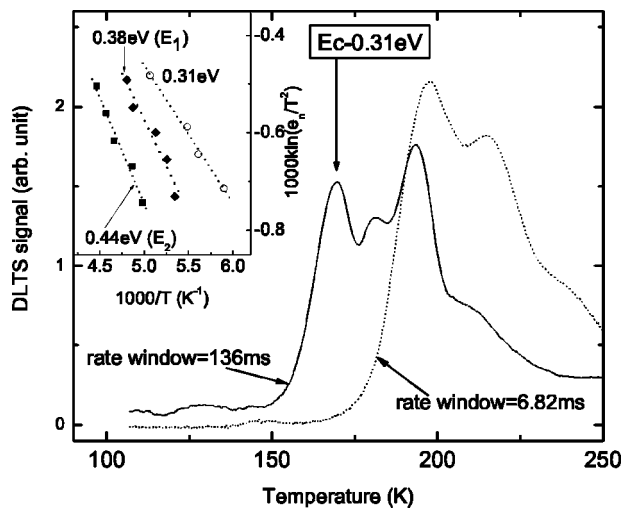


FIG. 4. DLTS spectra for the 900 °C annealed He-implanted sample with $V_r = -2$ V, rate window = 136 ms and filling pulse $t_p = 100$ μ s. The proposed peak causing the anomalous parameters of E_1/E_2 is highlighted by arrow. The inset shows the Arrhenius plots for E_1/E_2 and the new defect.

window = 6.82 ms) because increasing the rate window shifts the peaks to low temperature and this peak moves with a faster pace. With the Arrhenius plot, the activation energy and the cross section of this deep level were, respectively, found to be $E_C - 0.31$ eV and 8×10^{-14} cm². It is also worth pointing out that great care should always be taken while studying the annealing behavior of E_1/E_2 , as the annealing of this defect at about 1000 °C could be misinterpreted as the drop of the E_1/E_2 intensity. The exact detail of this defect's microstructure is not known as DLTS does not offer direct information about the defect's microstructure. It was reported that the defect induced by the 0.3 MeV electron irradiation should be a primary defect involving the displace-

ment of the C-atom in the SiC lattice [10] (i.e., isolated V_C , C_i , or $V_C C_i$). The $E_C - 0.31$ eV defect should not be related to these primary defects because it was not detected in the 0.3 MeV electron irradiated sample.

In conclusion, this work has revealed a new defect which exists in He implanted and high energy electron-irradiated samples and anneals out at about 1000 °C. This discovery accounts for the discrepancy with the intensity ratio and capture cross sections expected of E_1/E_2 being from the same defect at different equivalent sites.

This project was funded by the CERG, RGC (Project Nos. 7085/01P and 7103/02P) and the CRCG, HKU. X.D.C. would like to thank HKU for his PDF support. M.G. acknowledges support from the Grants of National Nature Science of China (No. 60076010).

¹H. Morkoç, S. Strite, G. B. Gao, M. E. Lin, B. Sverdlov, and M. Burns, *J. Appl. Phys.* **76**, 1363 (1994).

²T. Dalibor, G. Pensl, H. Matsunami, T. Kimoto, W. J. Choyke, A. Schoener, and N. Nordell, *Phys. Status Solidi A* **162**, 199 (1997).

³G. Pensl and W. J. Choyke, *Physica B* **185**, 264 (1993).

⁴C. G. Hemmingsson, T. N. Son, O. Kordina, E. Janzén, and J. L. Lindström, *J. Appl. Phys.* **84**, 704 (1998).

⁵M. Gong, S. Fung, C. D. Beling, and Z. P. You, *J. Appl. Phys.* **85**, 7604 (1999).

⁶M. O. Aboelfotoh and J. P. Doyle, *Phys. Rev. B* **59**, 10823 (1999).

⁷A. A. Lebedev, A. I. Veinger, D. V. Davydov, V. V. Kozlovski, N. S. Savkina, and A. M. Stel'chuk, *J. Appl. Phys.* **88**, 6265 (2000).

⁸A. Kawasuso, F. Redmann, R. Krause-Rehberg, T. Frank, M. Weidner, G. Pensl, P. Sperr, and H. Itoh, *J. Appl. Phys.* **90**, 3377 (2001).

⁹X. D. Chen, S. Fung, C. C. Ling, C. D. Beling, and M. Gong, *J. Appl. Phys.* **94**, 3004 (2003).

¹⁰X. D. Chen, C. L. Yang, M. Gong, W. K. Ge, S. Fung, C. D. Beling, J. N. Wang, M. K. Lui, and C. C. Ling, *Phys. Rev. Lett.* **92**, 125504 (2004).

¹¹I. Pintilie, L. Pintilie, K. Irscher, and B. Thomas, *Appl. Phys. Lett.* **81**, 4841 (2002).